Spectral-Interferometry Measurements of Copper Atom Concentration in a Segmented Hollow Cathode Discharge

L. Szalai, M. Ulbel[a], T. Neger[a], G. Pretzler[a], Z. Donkó, K. Rózsa, and R. C. Tobin[b]

Research Institute for Solid State Physics of the Hungarian Academy of Sciences, H-1525 Budapest, P.O. Box 49, Hungary

[a] Institut für Experimentalphysik, Technische Universität Graz, Petersgasse 16, A-8010 Graz, Austria

[b] Department of Physics, Monash University, Clayton, Melbourne, Victoria, 3168 Australia

Z. Naturforsch. **52a,** 771–777 (1997); received July 12, 1997

We report spectral-interferometry measurements of the concentration and the spatial distribution of copper vapor in a high voltage, segmented hollow cathode discharge, which is an efficient source for laser light generation. The concentration of sputtered copper atoms was found to be in the order of 10^{14} cm^{-3} at currents of 0.6–1.0 A in a 5 cm long, 4 mm bore diameter discharge tube, operating in argon buffer gas. At high pressures and relatively low current densities the sputtered metal concentration forms two maxima near the cathode surface. With increasing current and decreasing pressure these two maxima move towards the center of the discharge. This result may account for the fact that at certain discharge parameters the segmented hollow cathode lasers operate in higher order transverse modes near the threshold. The measurements of copper vapor concentration show increased sputtering compared to conventional hollow cathodes, which is considered to be one of the reasons for segmented hollow cathode metal ion lasers being more efficient.

Key words: Optical spectroscopy, optical interferometry, glow discharges, sputtering, gas lasers.

1. Introduction

Hollow cathode discharges provide an efficient way to excite metal ion laser transitions. The metal vapor is produced by cathode sputtering, and the laser transition is pumped by the thermal energy charge transfer reaction between the ground state positive ions of the buffer gas and metal atoms [1]. High voltage hollow cathode discharges – such as the newly developed segmented hollow cathode discharge (SHC) shown in Fig. 1 – exhibit higher stability and improved laser performance [2–4] compared to lasers operating in conventional (low voltage, slotted or cylindrical) hollow cathode discharges. The high gain provided by the SHC discharge makes it a possible pumping source for potential VUV laser transitions of Cu–II in the 150–170 nm wavelength range [1]. However, to achieve a gain which would be sufficient for this short wavelength range, several parameters of the discharge have to be optimized.

The excitation rate of metal ion laser transitions is proportional to the product of the ground state metal vapor density and the buffer gas ion density [1], *thus measurements of concentration and of the spatial distribution of the sputtered metal vapor is of basic importance for designing and optimizing the discharge constructions.* Apart from applications for lasers, glow discharges including sputtered metal vapor also play an important role in mass spectrometry [5] and spectroscopic light sources [6]. The presence of the sputtered cathode material in the discharge plasma can be studied by emission spectroscopy [7], absorption methods [8–10], laser induced fluorescence [11] and by spectral interferometry [12, 13].

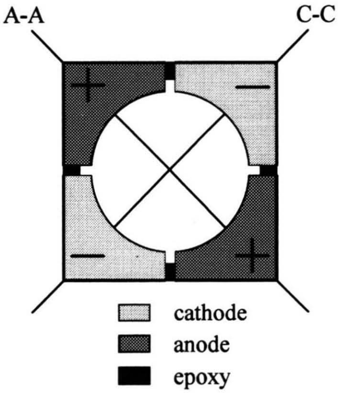

Fig. 1. Cross section of the segmented hollow cathode (SHC). The spatial distribution of the Cu atom concentration was measured along the cathode–cathode (C–C) and anode–anode (A–A) sections.

Reprint requests to L. Szalai, e-mail: lszalai@sunserv.kfki.hu

0932-0784 / 97 / 1100-0771 $ 06.00 © – Verlag der Zeitschrift für Naturforschung, D-72027 Tübingen

Absorption techniques based on the change of the intensity of the transmitted light through the plasma have already been applied to determine the spatial distribution of the metal vapor density in laser-purpose hollow cathode discharges [8, 9]. On the other hand, the spatial distribution of metal vapor concentration has not yet been investigated in the SHC discharge, and the only data for copper vapor concentration are available from spatially averaged time – resolved absorption measurements [10]. SHC discharges are characterized by voltage – current curves which exhibit a much higher slope than conventional hollow cathode discharges and operate at voltages in the 500 V–1000 V range. Therefore the sputtering is more efficient compared to conventional hollow cathodes due to the higher ion energies in the SHC discharge. As the increase of current in the SHC is accompanied by a significant increase in voltage, the concentration of sputtered metal is expected to increase faster with the current than in conventional hollow cathode discharges. Since the sputtered metal has an easy access into the plasma volume, the metal vapor concentration should be higher than in other high voltage hollow cathode constructions such as the hollow-anode-cathode discharge [14]. Also, due to the special electrode arrangement, the density distribution of the sputtered metal has neither cylindrical symmetry (like in a cylindrical hollow cathode [8]) nor a one dimensional dependence (as in a plane-parallel hollow cathode]), but it is expected to have a different spatial distribution between the cathode and anode segments. Due to the special electrode arrangement, the distribution of sputtered metal cannot be deduced from the data obtained in cylindrical and plane-parallel hollow cathodes.

Copper ion lasers are pumped by thermal charge transfer from He ions (780.8 nm) or by Ne ions (e.g. 248.6 nm), and a small percentage of Ar is often included to assist the sputtering (e.g. He + 4% Ar at a total pressure of 10–25 mbar). The present work concerns the spatial variation of ground state Cu in a SHC discharge in Ar at a pressure in the range 2–4 mbar. In the He + Ar mixture used in the lasers, the Ar^+ ions play an important role in producing the copper atoms by sputtering. Thus, as in the pure argon discharge the dominant particles for sputtering are also Ar^+ ions, the results obtained for the argon discharge are useful for the understanding of discharge processes in the He + Ar discharges as well.

The method used in our present measurements – spectral interferometry – utilizes the density dependent change of the refractive index in the vicinity of spectral lines to determine particle concentrations [12, 13]. In the interferometer a white light interferogram is formed and the particle concentration can be determined from the distortion of the interference patterns near the spectral lines. This method has already been used successfully for the diagnostics of different types of gas discharges [13]. The advantages of the method are its accuracy, high spatial resolution, and that the spatial distribution of the particle density along one transverse direction in the discharge can be recorded *simultaneously*, during a short time of discharge operation.

Our results indicate that the segmented hollow cathode discharge provides more efficient sputtering than the conventional hollow cathode discharges, which is advantageous for cathode sputtered metal ion lasers.

In Sect. 2 we describe the experimental apparatus and briefly summarize the basics of spectral interferometry. The results of our measurements are presented and discussed in Sect. 3 and summarized in Sect. 4, respectively.

2. Experimental Setup and Data Evaluation

The experimental setup used in our measurement of atomic copper densities in the segmented hollow cathode (SHC) discharge is shown in Figure 2. The investigated discharge tube was situated in the 85 cm long test – arm of a Mach – Zehnder interferometer. The beamsplitters (BS1 and BS2) and the mirrors (M1 and M2) had 50 mm diameter. The L1, L2, and L3 lenses and the M3 and M4 mirrors were aligned using a He-Ne laser. The interference pattern, localized in the center of the discharge is imaged onto the entrance slit of a Jobin Yvon HR1000 spectrograph. The illuminating light source used for our measurements was a capillary discharge emitting a strong radiation over the whole ultraviolet and visible wavelength range. The discharge was established between two graphite electrodes in a 1 mm hole drilled in a 5 mm thick plastic plate. The interferograms were recorded on a photographic plate positioned at the exit plane of the spectrograph (cf. Figure 3).

The measurements were carried out using argon buffer gas in order to have a sufficiently high sputter-

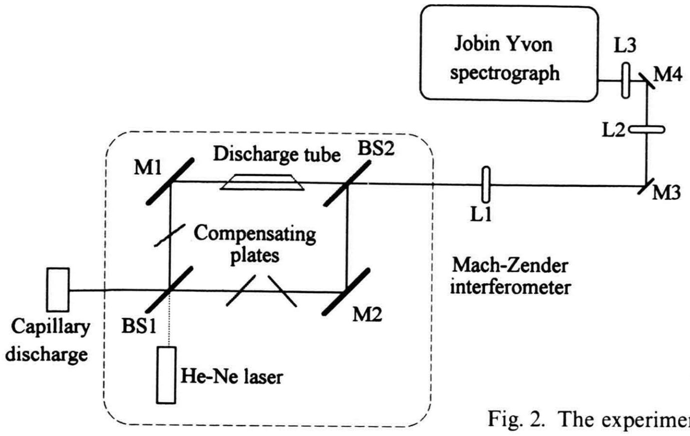

Fig. 2. The experimental setup of spectral interferometry measurements.

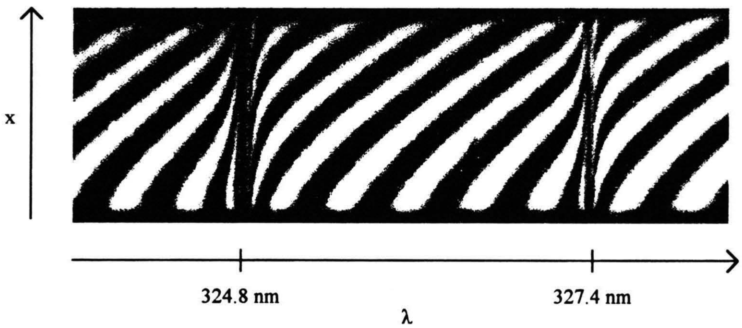

Fig. 3. Spectral interferometric recording in the vicinity of the Cu–I resonance lines. Discharge conditions: $p=3$ mbar, $I=1$ A.

ing rate of the cathode material. A slow flow of the gas was applied to maintain cleanliness of the discharge tube. The current pulses applied to the tube were approximately 1 sec long, to approach DC conditions. The discharge tube was water-cooled to avoid overheating. The range of currents employed was 0.6–1.0 A, resulting in 0.2–0.35 A/cm^2 current density on the cathode surface. The argon pressure was in the range of 2–4 mbar.

The cross section of the segmented hollow cathode discharge used in our measurements is plotted in Figure 1. The discharge tube was 5 cm long and had 4 mm inner diameter. The electrodes were made of high purity, oxygen free (OFHC) copper. The electrodes were separated by thin ceramic spacers to maintain a 0.3 mm gap between them. Durol type 15 epoxy resin was used to glue the electrodes together.

The spectral lines used for the spectral interferometry were the 324.8 nm and 327.4 nm resonance lines of Cu–I. After the measurements the interferometric recordings were digitized and evaluated using computer programs developed for this purpose [13]. The evaluation of the interferograms was based on a two-dimensional Fast Fourier Transform [15]. The interference fringes were transformed into the frequency domain. Applying proper filtering and executing the inverse FFT transform, the spatial distribution of the Φ phase of interfering waves (depending on the λ wavelength and the x position along the measured direction) is obtained:

$$\Phi(\lambda, x)=2\,\pi\,k(\lambda, x)=\arctan\frac{\mathrm{Im}\,[I_{\mathrm{F}}(\lambda, x)]}{\mathrm{Re}\,[I_{\mathrm{F}}(\lambda, x)]}, \qquad (1)$$

where $I_{\mathrm{F}}(\lambda, x)$ is the spatial dependence of the frequency-filtered intensity. Using this phase information, the particle concentration can be calculated from

$$k(\lambda, x)=A(\lambda, x)+\frac{r_0}{2\pi}\,N(x)\,f_{ik}\,L\,\frac{\lambda_{ik}^2\,\lambda}{\lambda^2-\lambda_{ik}^2}, \qquad (2)$$

where $A(\lambda, x)$ is known from the settings of the interferometer and does not depend on the sputtered atom concentration, r_0 is the classical electron radius, f_{ik} and λ_{ik} are the oscillator strength and wavelength of the '*ik*' transition, L is the length of the discharge and N is the concentration of examined particles. More details on the experimental apparatus and data acquisition can be found in [13].

Our results for the Cu atom concentration are presented for the cathode–cathode and anode–anode sections of the SHC discharge (see Figure 1).

3. Results and Discussion

The metal vapor density measurements were carried out at different discharge conditions to study the effect of the gas pressure and discharge current.

As an illustration of the method of the measurement, Fig. 3 displays one of the recorded interferograms, for discharge conditions $p = 3$ mbar pressure and 1.0 A current. The distortion of the interference fringes near the vicinity of the two resonance lines of Cu–I is clearly visible in the (λ, x) plane. We note that the oscillator strength of the 324.8 nm transition is twice the value of that of the 327.4 transition. Therefore the phase distribution near the 324.8 nm line was used for the evaluation of the concentration, as the higher oscillator strength results in higher sensitivity (see. eq. (2)).

Figures 4 and 5 show the $N(x)$ spatial distribution of Cu atom concentration in the cathode–cathode and anode–anode sections of the discharge, respectively, for $p = 3$ mbar and currents between 0.7 and 1.0 A. It can be seen that at constant pressure the average concentration of sputtered metal increases with increasing discharge current. The measurements in the cathode–cathode section (Fig. 4) indicate that the maximum concentration of Cu atoms can be found at approximately 0.5 mm distance from the cathode walls. The position of the peaks of $N(x)$ move slightly towards the center of the discharge with increasing current. It can also be seen in Fig. 4 that the copper concentration in the center of the discharge increases ≈ 1.5 times faster with increasing current than the peak value of $N(x)$. The progressively more uniform distribution of copper in the central region of the discharge at higher currents is favourable for the laser operation. The copper concentration in the axis of the discharge in Figs. 4 and 5 (obtained from the measurements in the C–C and A–A sections, respectively) agrees well for the currents 0.7 A and 0.8 A. At higher currents, however, higher density was obtained in the measurements in the A–A section. These values are still in reasonable agreement with each other considering the estimated $\pm 10\%$ accuracy of the mea-

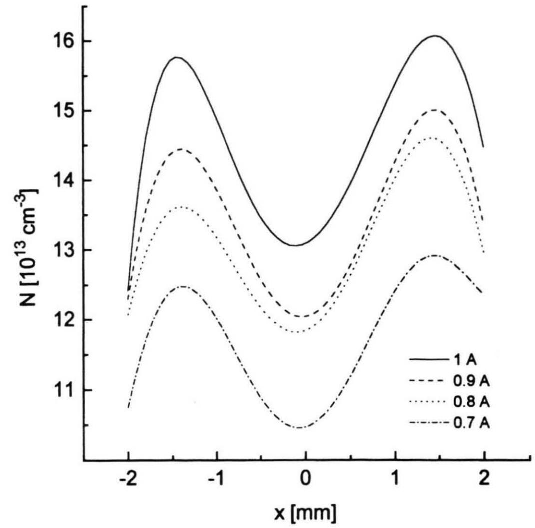

Fig. 4. The $N(x)$ density distribution of Cu atoms in the cathode–cathode (C–C) section of the discharge at 0.7–1.0 A discharge current, for 3 mbar argon pressure (Note that Figs. 4–8 show only the needed part of the ordinate).

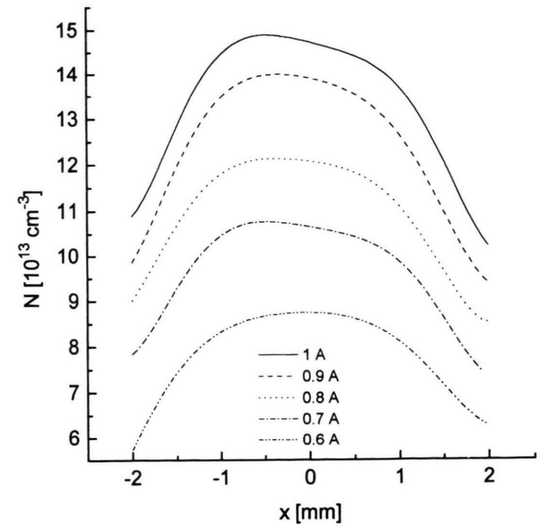

Fig. 5. The $N(x)$ density distribution of Cu atoms in the anode–anode (A–A) section of the discharge at 0.6–1.0 A discharge current, for 3 mbar argon pressure.

surement (also including repeatability of the discharge pulses and errors of data acquisition).

The typical shape of the $N(x)$ curves such as shown in Fig. 4 can be explained by the following discharge mechanisms. The bombardment of energetic heavy particles (fast Ar^+ ions and fast Ar atoms) result in the ejection of copper atoms from the surface with a typical energy of several eV. These sputtered fast atoms thermalize via collisions with buffer gas atoms as they proceed towards the center of the discharge. The thermalization can be considered complete when the temperature of copper atoms is equal to the background gas temperature. The motion of the thermalized atoms is governed by diffusion. The surfaces of electrodes act as sinks and in some buffer gases the copper atom concentration is also depleted by the thermal charge transfer (laser-pumping) process.

In the anode–anode section (Fig. 5) the concentration is low near the anodes (as they act as perfect sinks for the metal vapor). The distribution in the anode–anode section has a quite flat maximum around the axis of the discharge.

The values of Cu atom concentration agree well with the spatially averaged copper concentration (obtained by absorption technique) obtained in [10]. For example, the average Cu concentration was found to be 7×10^{13} cm^{-3} at 1 A (≈ 0.3 A cm^{-2} current density) current and 12.5 mbar pressure, in He+4% Ar mixture [10]. In our similar SHC discharge tube the average copper concentration is approximately 30–40% higher, at the same current of 1 A, at 3 mbar argon pressure. Previous absorption measurements and calculations of *spatial distribution* of copper vapor have been carried out for neon buffer gas for cylindrical [8] and plane-parallel [9] hollow cathodes. In [8] peak copper densities in the order of 6×10^{13} cm^{-3} were reported, for current densities ≈ 0.1 A cm^{-2}. In plane-parallel hollow cathodes peak concentrations up to 1.3×10^{14} cm^{-3} have been obtained for 0.2 A cm^{-2} current density [9]. In this case the separation of the cathodes was 2 mm, which is about half the distance of cathodes in our SHC discharge. Thus comparing our results with those, it is obvious that in a smaller, e.g. 2 mm diameter SHC discharge a significantly higher metal vapor concentration can be expected. Although the sputtering coefficients of argon are somewhat higher than that of neon, we can conclude that the segmented hollow cathode discharge provides more efficient sputtering than the conventional (cylindrical or slotted) hollow cathodes. This leads to lower threshold current and increased gain of metal ion lasers operating in SHC discharges [1–4] and thus is considered to be one of the reasons for their more efficient operation.

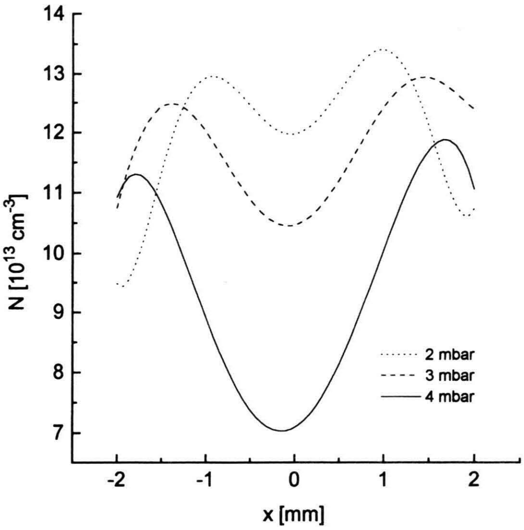

Fig. 6. The $N(x)$ density distribution of Cu atoms in the cathode–cathode (C–C) section of the discharge at $p=2$, 3 and 4 mbar argon pressure, for $I=0.7$ A.

The spatial distribution of copper atom density in the segmented hollow cathode discharge, along the cathode–cathode section is displayed in Fig. 6 for different buffer gas pressures and for a fixed current of $I=0.7$ A. It can be seen in Fig. 6 that with decreasing pressure the peaks of $N(x)$ move towards the center of the discharge. The average Cu concentration also increases with decreasing pressure and an increased copper density can be obtained in the center of the tube. It can also be seen that with increasing pressure the dip in the distribution in the middle of the discharge gets deeper, as it is less probable that the copper atoms reach the center.

Figure 7 shows the dependence of the copper concentration in the center of the discharge for different pressures. It can be seen that the concentration increases with decreasing pressure. As the dip in the $N(x)$ distribution at lower pressures is less than at high pressures, the concentration at the axis increases slowly with current at lower pressure. At higher pressure (4 mbar) the dip at the axis is being filled due to the moving of the two peaks towards the center of the discharge at this results in a relatively higher rate of change of $N(x=0)$ with current.

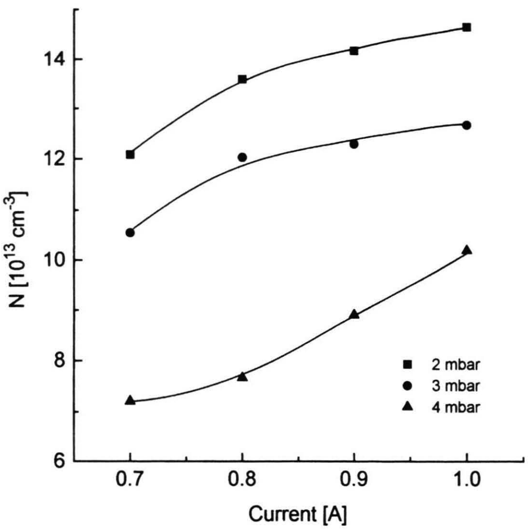

Fig. 7. The Cu atom concentration in the middle of the discharge versus the discharge current at $p=2$, 3 and 4 mbar argon pressure.

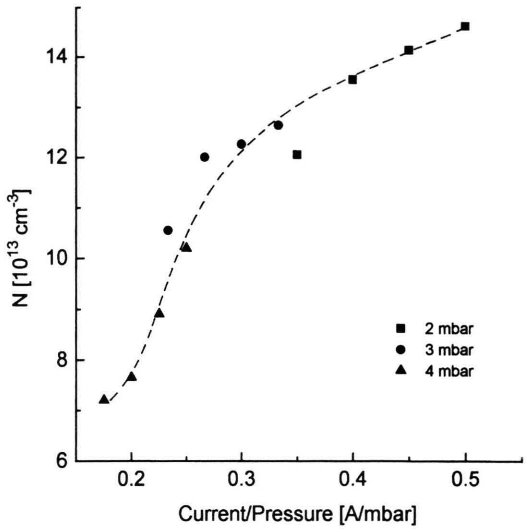

Fig. 8. The Cu atom concentration in the middle of the discharge versus the discharge current to argon pressure ratio.

We have found that the values of Cu concentration plotted as a function of the current (I) to pressure (p) ratio closely (within the estimated accuracy of $\pm 10\%$) lie on a universal curve, shown in Figure 8. The reason of this 'universal' relationship has not yet been clarified. However, we note that the discharge voltage of the SHC was found to scale with the I/p ratio [2]. The similar behaviour of copper atom concentration may be attributed to the fact that the sputtering rate has a strong dependence on the energy of ions bombarding the cathode, which is influenced by the discharge voltage.

Since the excitation rate of metal ion lasers is proportional to the product of the ground state metal atom concentration and the buffer gas ion concentration, it is important to investigate the behaviour of sputtered metal in hollow cathode discharges. As we have carried out our measurements in argon gas and in a different pressure range than that used in metal ion laser, our result can only be connected qualitatively to the properties of metal ion lasers. Our results indicate that the pumping rate may vary considerably in the cross section of the SHC discharge. This may give rise to different than TEM_{00} transversal mode operation. Higher order transversal modes have already been found to have highest gain (lowest threshold current) in an SHC discharge [16]. The other important species in the pumping of the metal ion lasers, the buffer gas ions were found to have a sharply peaked source function [17] and consequently a density distribution with a maximum around the discharge axis [18] in SHC discharges. Measurements on the spatial distribution of small signal gain of the 780.8 nm He–Cu^+ laser have confirmed that at low buffer gas pressures the gain is peaked at the axis of the discharge and at higher pressure the small signal gain has two maxima off-axis [19].

4. Conclusions

We have applied spectral interferometry to investigate the dependence of the concentration and spatial distribution of sputtered metal on the buffer gas (Ar) pressure and discharge current in a segmented hollow cathode discharge. The spatial distribution of metal vapor is consistent with the gain distribution of metal ion laser lines in the cross section of the discharge.

We have shown that

(i) in the cathode–cathode section of the discharge the metal vapor concentration has two peaks near the cathode surface (similarly to plane-parallel hollow cathodes [9]),

(ii) the position of the peaks of the metal vapor concentration move towards the center of the discharge with decreasing pressure and also with increasing current,

(iii) with increasing current the metal vapor concentration on the axis increases faster than the peak concentration.

(iv) in the anode–anode section of the discharge, the maximum concentration is always found on the discharge axis and exhibits a broad maximum.

The typical peak metal vapor concentration was found to be in the order of $1-1.5\times10^{14}$ cm^{-3} for a discharge current in the order of 0.6–1.0 A in our 5 cm long SHC tube. The data obtained in our measurements can be used for future optimization of the discharge construction and also for validation of models of the SHC discharge [18]. Comparing the present concentration data with data obtained in conventional (cylindrical or slotted) hollow cathode discharges, we can conclude that the segmented hollow cathode discharge provides more efficient sputtering of the cathode material. This is considered to be one of the reasons leading to the more efficient operation of SHC discharge metal ion lasers.

The study reported here is a part of the diagnostics and optimization of high voltage hollow cathode discharges aimed at more efficient ultraviolet laser light generation and the demonstration of continuous vacuum-ultraviolet laser action in copper vapor.

Acknowledgements

This work was supported by the CEEPUS Network A-8 and by the Hungarian Science Foundation (OTKA) Grants No. F-025503, T-14909 and F-15502. We thank Dr. M. Jánossy for helpful discussions and his suggestions on the manuscript. The construction of the discharge tube by T. Judit Forgács, J. Tóth, E. Sárközi, and Gy. Császár is gratefully acknowledged.

[1] R. C. Tobin, K. A. Peard, G. H. Bode, K. Rózsa, Z. Donkó, and L. Szalai, J. Selected Topics in Quantum Electronics **1,** 805 (1995).
[2] K. A. Peard, K. Rózsa, and R. C. Tobin, J. Phys. D: Appl. Phys. **27,** 219 (1994).
[3] K. A. Peard, Z. Donkó, K. Rózsa, L. Szalai, and R. C. Tobin, IEEE J. Quantum Electronics **30,** 2157 (1994).
[4] K. A. Peard, R. C. Tobin, K. Rózsa, and Z. Donkó, IEEE J. Quantum Electronics **30,** 1181 (1994).
[5] A. Bogaerts, M. van Straaten, and R. Gijbels, Spectrochim. Acta **50 B,** 179 (1995).
[6] A. Walsh, Spectrochim. Acta **7,** 108 (1955), P. Apai, and K. Rózsa, Hollow cathode laboratory light sources, in Proc. of EPCLP'91 Pentagonale Workshop on Elementary Processes in Clusters, Lasers and Plasmas, April 8–12, 1991, Kühtai 1991, Austria, p. 286.
[7] Z. Wroński, J. Sielanko, and J. L. Sullivan, J. Phys. D: Appl. Phys. **29,** 1509 (1996).
[8] E. M. van Veldhuizen and F. J. Hoog, J. Phys. D: Appl. Phys. **17,** 953 (1984).
[9] J. R. McNeil, PhD Thesis, Colorado State University (1978), B. E. Warner, K. B. Persson, and G. J. Collins, J. Appl. Phys. **50,** 5694 (1979).
[10] K. A. Peard, PhD Thesis, Monash University, Australia (1994).
[11] A. Bogaerts, E. Wagner, B. W. Smith, J. D. Winefordner, D. Pollmann, W. W. Harrison, and R. Gijbels, Spectrochim. Acta **52 B,** 205 (1997).
[12] W. C. Marlow, Appl. Opt. **6,** 1715 (1967), M. C. E. Huber, Interferometric gas diagnostics by the hook method, in Progress in Gas Dynamic Research by Optical Methods (ed. D. S. Dosanjh, New York 1971, Plenum).
[13] R. Sperger and T. Neger, Opt. Commun. **80,** 401 (1991); T. Neger, Habilitationsschrift, Technical Univ. Graz 1993.
[14] K. Rózsa, Z. Naturforsch. **35a,** 649 (1980).
[15] M. Takeda, H. Ina, and S. Kobayashi, J. Opt. Soc. Amer. **72,** 156 (1982).
[16] B. L. Leigh, R. C. Tobin, K. Rózsa, and Z. Donkó: Dependence of gain output power on cathode to anode area ratio in a segmented hollow-cathode Cu-II 781 nm laser, J. Phys. D: Appl. Phys. to be published (1997).
[17] Z. Donkó, K. Rózsa, and R. C. Tobin, J. Phys. D: Applied Physics **29,** 105 (1996).
[18] R. R. Arslanbekov and R. C. Tobin, A. A. Kudryavtsev: J. Appl. Phys. **81,** 554 (1997).
[19] T. M. Adamowicz, Z. Donkó, L. Szalai, K. Rózsa, and W. Kwaśniewski, The spatial distribution of small signal gain in a segmented hollow cathode discharge laser, Appl. Phys. B, to be published (1997).